

Received March 6, 2020, accepted March 22, 2020, date of publication March 30, 2020, date of current version April 14, 2020.

Digital Object Identifier 10.1109/ACCESS.2020.2983907

Various Aging Processes in a Paper-Natural Ester Insulation System in the Presence of Copper and Moisture

PAVEL TRNKA¹, (Senior Member, IEEE), JAROSLAV HORNÁK¹, (Member, IEEE),
PAVEL PROSR¹, (Member, IEEE), ONDREJ MICHAL¹, (Member, IEEE),
AND FEIPENG WANG², (Member, IEEE)

¹Faculty of Electrical Engineering, University of West Bohemia, 30100 Pilsen, Czech Republic

²Department of High Voltage and Electrical Insulation, School of Electrical Engineering, Chongqing University, Chongqing 400044, China

Corresponding author: Pavel Trnka (pavel@ket.zcu.cz)

This work was supported by the Ministry of Education, Youth and Sports of the Czech Republic through Project OP VVV Electrical Engineering Technologies with High-Level of Embedded Intelligence under Grant CZ.02.1.01/0.0/0.0/18_069/0009855.

ABSTRACT This article adds more information to the problem of natural ester use as an electroinsulating fluid in cellulose paper-oil systems, e.g., for use in power transformers. An accelerated thermal aging (120, 140 and 160 °C) of samples consisting of cellulose paper (transformerboard), a treated natural ester (filtered, basic Al₂O₃, 0.53% DBPC), a copper plate and moisture was studied. Research was especially focused on the impact of moisture on the aging of the above system. Samples with three different oil moisture levels (80, 143 and 305 ppm water content) were subjected to thermal aging to display the change in a selection of properties (tan δ , acid number, water content). For a study of the polarization effects, broadband dielectric spectroscopy (BDS) was performed to observe the complex permittivity and conductivity dependencies on the temperature and frequency (± 30 °C, 0.01–10⁷ Hz). Havriliak-Negami (H-N) diagrams were used to further understand the results. The degradation products during thermal aging were recognized by Fourier transform infrared (FT-IR) spectroscopy. Hydrolysis and hydrogenation occurred in the insulating system with a natural ester aged by elevated temperatures, which is in contrast to CO₂ formation in the case of electric aging. The results showed an increase in the acid number, dissipation factor, and number of hydrolysis and hydrogenation products. Furthermore, changes in polarization were observed as a consequence of the thermal aging of paper-natural ester insulation system with the presence of copper and moisture.

INDEX TERMS Aging, dielectrics, hydrogenation, hydrolysis, oil insulation, paper-oil insulating system, natural ester, complex permittivity.

I. INTRODUCTION

Studies related to the use of natural ester fluids as an intended replacement of mineral oil in paper oil insulation systems have been conducted and published many times, e.g., in [1]–[3]. Often mentioned problems are the higher viscosity of esters, up to 50 mm²·s⁻¹ at 40 °C [4]; higher pour point, –17––28 °C [5]; higher permittivity, $\epsilon_r = 3$ –4 [6]; lower oxidative stability [7]; and higher price of commercially produced esters compared with those of mineral oils. These facts play a critical role in the current deployment of ester fluids in industry. Less well-known are the problems of

inadequate legislation (standards-defined operational limits) that make the wider industrial use of natural esters more demanding, along with durability problems in terms of lower lightning impulse (LI) resistance [8], [9], oxidative stability, etc. Esters and natural esters also have many benefits, e.g., a low degree of cellulose polymerization (in the system) compared to mineral fluids [10], a high flash point and fire point [11] and a relatively high “moisture tolerance” of its dielectric properties [12], higher permittivity is prone a better electric field distribution in the paper-oil system [42] and esters have better thermal stress performance [43]. However, the moisture effect on the aging of the paper-natural ester oil system has not been deeply studied in terms of its degradation and the specific chemical reactions.

The associate editor coordinating the review of this manuscript and approving it for publication was Rajeswari Sundararajan.

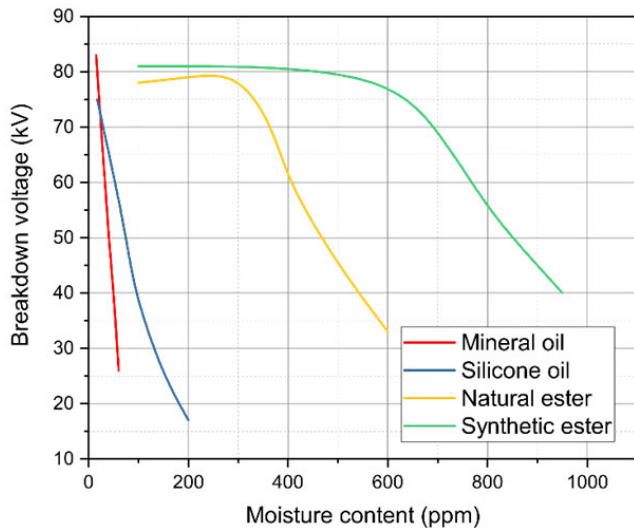


FIGURE 1. Moisture saturation of different dielectric fluids (redrawn from [14]).

With the consideration of a wider use of natural ester fluids, e.g., in high voltage machinery, users will require a proper user's manual with set limits for the monitored parameters. In current industrial practice, standards are defined as limits for certain parameters (paper-mineral oil system, e.g., IEC 60076-7, IEEE C57:100, ASTM D-982). The current industrial standards roughly define limits for certain parameters, which is extremely insufficient. For natural esters, some of the parameters are defined in IEC 62770 "Fluids for electrotechnical applications - Unused natural esters for transformers and similar electrical equipment" [13], others are being defined in the future IEC 62975 "Natural esters - Guidelines for maintenance and use in electrical equipment" as an equivalent of EN 60422 and a new project "Gas chromatographic analysis and evaluation of ester insulating liquids in electrical equipment" as an equivalent of EN 60567.

The water content is a highly concerning parameter in regard to insulating liquids [15]. Ten to thirty ppm is the range in water content when mineral oils are used. The moisture levels of natural ester oils are on a different level due to the different chemical compositions of esters. Natural esters are composed of a glycerol backbone and fatty acids [16]. These fatty acids contain a high number of ester linkages that should attract water due to the high polarity of water. This result indicates that a high water content is acceptable by the ester oil. This has been evidenced by the very relaxed moisture-content dependence of the breakdown voltage (BDV) values in Figure 1.

CIGRE standard 436 – "Experiences in Service with New Insulating Liquids" states that the water saturation for natural esters is 1100 ppm compared to 55 ppm for mineral oil [14]. This CIGRE standard confirms the effect of moisture on the breakdown voltage value.

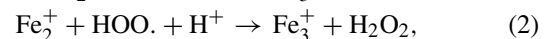
The acid number of the oil is used as an indicator of paper hydrolysis in paper-mineral oil systems. The reason for the increase in the acid number during aging of a paper-oil system

is that the molecular composition of cellulose consists of a long series of glucose molecules linked together [17]. When water is present - the hydrolysis of cellulose - glucose is released into the oil [18]. Catalysts [19] help to accelerate the process. A number of catalysts may act in the paper-oil degradation process; however, only one catalyst, copper, is intentionally used in the following test. Theoretically, the cellulose enzyme can also act as a catalyst (enzymatic hydrolysis). When an acid acts as the catalyst, we label it acid hydrolysis. Acid hydrolysis occurs in cellulose, and the resulting acid is dissolved in the oil [20].

The aim of this paper is to provide insight into the behavior of rapeseed oil aged with cellulose (paper, transformer-board) and copper at elevated temperatures and with different moisture levels; in particular, a different aging mechanism that occurs due to the different chemical constituents of the resulting ester fluids is described.

II. CELLULOSE DEGRADATION PROCESSES

As mentioned above, the main degradation of cellulose is due to hydrolysis. However, more cellulose degradation processes can occur, e.g., initiated by the presence of excess Fe ions (magnetic core, transformer tank, and mechanical supports). This can catalyze the oxidation of cellulose through the production of hydrogen peroxide according to a Fenton mechanism [21], which is shown by equations (1) and (2):



This can also lead to a significant destruction of the paper, which has yet to be described, e.g., transformer diagnostics. As described below, the acid number and water content increase with aging due to cellulose hydrolysis. An overview of the possible cellulose degradation types is shown in Table 1. More details about these types of cellulose hydrolysis, as well as others can be found in [22]–[25].

TABLE 1. Overview of possible cellulose degradation reaction types [22]–[25].

| Chemical Reaction | Reactants | Products |
|----------------------|-------------------------------------------|------------------------------------------------|
| Thermal hydrolysis | cellulose + H ₂ O | D-glucose |
| Acid hydrolysis | cellulose + H ₃ O ⁺ | D-glucose |
| Alkaline hydrolysis | cellulose + base | low molecular weight products |
| Enzymatic hydrolysis | cellulose + cellulase | low molecular weight products |
| Oxidation | cellulose + O ₂ (T, hv) | partially oxidized and depolymerized cellulose |

In addition to the abovementioned reactions, other chemical reactions may occur in cellulose over time depending

on the presence of reactants and the surrounding environment. However, the most significant for the problem of oil transformer diagnostics is acid hydrolysis, which will be mentioned further in the paper.

III. DEGRADATION PROCESSES IN NATURAL ESTERS

Natural ester oils are formed by the reaction of natural oils with alcohols or esterification. Natural oils are obtained by pressing seeds of plants such as rape, soya, sunflower, olives, poppy, flax, and castor. Vegetable oils are largely nontoxic and biodegradable, and they can be tested according to OECD 301 [26]. In esterification, the OH groups of the carboxylic acids are replaced by an organic moiety of the formed alcohol (R) when the hydrogen is removed from the OH group. The above esterification results in the formation of an ester and water, and the chemical reaction is described in Figure 2.

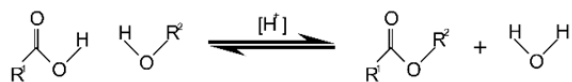


FIGURE 2. Process of the esterification of natural oil (redrawn and adapted from [27]).

As described above with cellulose paper, the technical life of natural esters depends on the raw materials from which they are made (internal factors) as well as the environment to which they are exposed (external factors). The major degradation processes of natural esters are hydrolysis [28], polymerization [29], oxidation [30], and hydrogenation [31].

IV. EXPERIMENT

The experiment was set up in order to gather data about the behavior of the paper-oil system with different water contents, where a liquid part was a treated natural ester-based oil [16] (rapeseed) with a 0.53% addition of dibutyl-para-cresol (DBPC). The parameters of the used oil are shown in Table 2. The cellulose part was represented by a

TABLE 2. Natural ester-based oil parameters, also in [16].

| Parameter | Value |
|--------------------------------|------------------------------------------|
| Appearance | clear without sediments and suppression |
| Density (20 °C) | 0.915 g·cm ⁻³ |
| Specific heat capacity (60 °C) | 1998 J·kg ⁻¹ ·K ⁻¹ |
| Viscosity (40 °C) | 35.84 mm ² ·s ⁻¹ |
| Pour point | -24 °C |
| Acid number | 0.011 mg KOH/g |
| Water content | 45 ppm |
| tanδ (90 °C) | 0.00358 |

transformerboard, and the transformer winding was replaced by a copper plate.

In technical applications, the electrical insulation system in the transformer is subject to temperatures up to approx. 90 °C for decades. In the experiment, time was replaced by accelerated aging with temperature, as described in ANSI/IEEE C57:100, IEC 60076.7. The experiment was conducted at three temperatures and three different water contents. Two exposure times were applied (Table 4) for each temperature (based on pre-test and recommendations of IEC 60216-6 and IEC 60505). To evaluate the experiment, the non-electrical parameters of the water content and acidity of the samples after exposure and the electrical parameters of the loss factor, permittivity and resistivity of the samples for temperatures from 30 °C to 90 °C were measured. Infrared spectroscopy was used to evaluate the processes occurring in the oils.

A. SAMPLE PREPARATION

In this experiment, samples of treated rapeseed oil (100 ml) were used with a transformer board (20 × 20 × 0.5 mm) and copper sheet (0.1 × 3 × 28 mm) to partially simulate the effects of individual parts of an insulation system on the oil properties. The water content of the oil at the start point of our test was 92 ppm, and the acid number was 0.01 mg KOH/g. Each sample (oil + paper + copper) was placed in a 100-ml dark and sealed reagent bottle with a narrow neck and ground cap. The oil:copper:paper (ambient) weight ratio was approximately 915:75:0.24 g, which was equivalent to 92:7.5:0.02%. The presence of air during the accelerated thermal aging was eliminated.

Three types of samples with different water contents were prepared. The water was delivered to the system via a transformerboard. In the first type, the paper insulation (sample marked as “ambient”) was exposed to an ambient environment that was 23 °C and 47% RH for 168 hours. The second paper insulation (sample marked as “dry”) was dried for 24 hours at 85 °C. The last sample was wet paper insulation (sample marked as “wet”), which was exposed in a climatic chamber for 24 hours at 40 °C and 70% RH. The resulting gain of water weight was 0.02272 g (9.5%) in the wet samples and the loss of water weight was 0.03734 g (-15.65%) in the dry samples. A representative of each “moisture”-type sample was then exposed to an elevated temperature. Four sets of three samples with different (3 levels) moisture contents were prepared. Exposure parameters are summarized in Table 3.

TABLE 3. Transformerboard exposure parameters.

| Sample | Temperature (°C) | Relative humidity (%) | Time (hours) |
|---------|------------------|-----------------------|--------------|
| DRY | 85 | - | 24 |
| AMBIENT | 23 | 47 | 168 |
| WET | 40 | 70 | 24 |

TABLE 4. Sample temperature and exposure time.

| Sample | Temperature (°C) | Exposure Time (hours) |
|----------|------------------|-----------------------|
| T1 short | 160 | 800 |
| T1 long | 160 | 1200 |
| T2 short | 140 | 1000 |
| T2 long | 140 | 1500 |
| T3 short | 120 | 1600 |
| T3 long | 120 | 2000 |

Next, the samples were exposed to three accelerated aging temperatures T1 - T3 (120, 140, 160 °C, respectively) and different exposure times marked as “long” and “short”, see Table 4. Thus, each sample was described by the temperature, exposure time and humidity of the board, for example 160 °C, short, dry (measured through the water dissipated in oil). It was necessary to start the heat exposure immediately after the insertion of the paper and the copper slices into the oil bottles.

The measurement followed the thermal exposure as soon as possible. The measurement procedures are described in the following chapters.

B. WATER CONTENT AND ACID NUMBER MEASUREMENT

The water content of the oil samples was measured by Coulometer WTD (Diram) based on a Karl Fischer titration. The same device was used for an acid number measurement based on the coulometric determination of alkali blue B6 as a spectrophotometric indicator.

C. DISSIPATION FACTOR AND PERMITTIVITY MEASUREMENT

The dissipation factor is an indicator of the quality of the electrical insulation material, and it represents losses that occur in the dielectric material. The measurement of the dissipation factor was performed by a Tettex 2830/2831 dielectric analyzer along with a suitable 2903 electrode system (both Haefely). The dissipation factor was measured at a voltage of 500 V, a frequency of 50 Hz and a temperature range of 30 to 90 °C.

Since the dissipation factor is an industrial parameter, the complex permittivity versus temperature and frequency of the paper insulation was measured using broadband dielectric spectroscopy after the accelerated thermal exposure. For this investigation, the main diagnostic unit of an Alpha-A measuring device (Novocontrol Technologies) was used. It contained a frequency response analyzer and electrode system whose sample cell consisted of two parallel cylindrical gold-plated electrodes, and the flat sample to be tested was placed between these electrodes. The measurement of the loss factor

and permittivity of the aged oil transformerboard was carried out at temperatures of −30 to 30 °C with a step of 10 °C. For each temperature, spectroscopy was performed in a range of 0.01 Hz to 10 MHz.

D. FOURIER TRANSFORM INFRARED SPECTROSCOPY

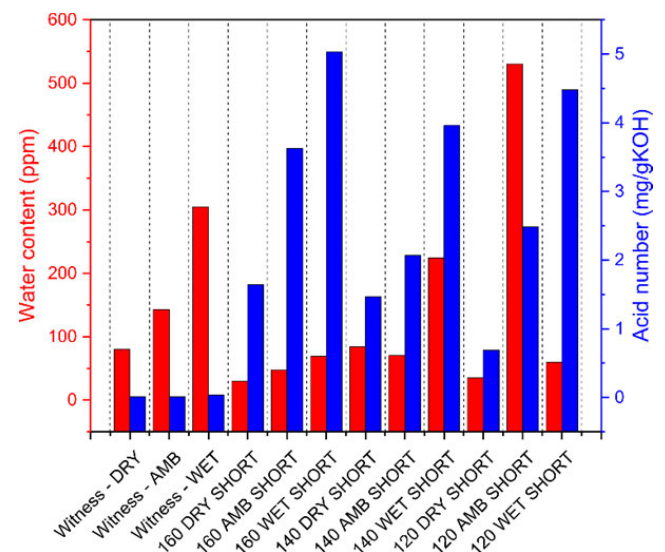
Fourier transform infrared (FT-IR) spectroscopy measurements were carried out with a Nicolet 380 spectrum analyzer (Thermo Scientific) in the middle region of the infrared spectrum with the use of PIKE demountable liquid cell kits with BaF₂ windows (an optical path of 1 mm). The spectra were acquired at a 1 cm^{−1} resolution with a total of 32 scans co-added for each measured spectrum. Every oil sample was filled and collected with a count of 3 (i.e., measurement frequency, n=3) and statistically averaged using Omnic spectroscopic software. All measurements were performed at the end of the thermal exposure.

V. RESULTS AND DISCUSSION

In the following, the results of the experiment are presented, and the observed mechanisms are discussed.

A. WATER CONTENT AND ACID NUMBER

The resulting values of the water content and acid numbers are presented in Figure 3 and Figure 4. The moisture content resulted from the three humidity levels during the paper preparation (subjected to ambient conditions - ambient, dried in the oven - dry, and climatic chamber - wet) and a natural ester with an initial water content of 92 ppm. The resulting moisture level is the result of the paper and oil degradation within the paper-oil samples (hydrolysis and hydrogenation).

**FIGURE 3.** Comparison of water content and acid number for each SHORT sample.

Witness samples were prepared using the same procedure and measured after 800 hours at an ambient temperature.

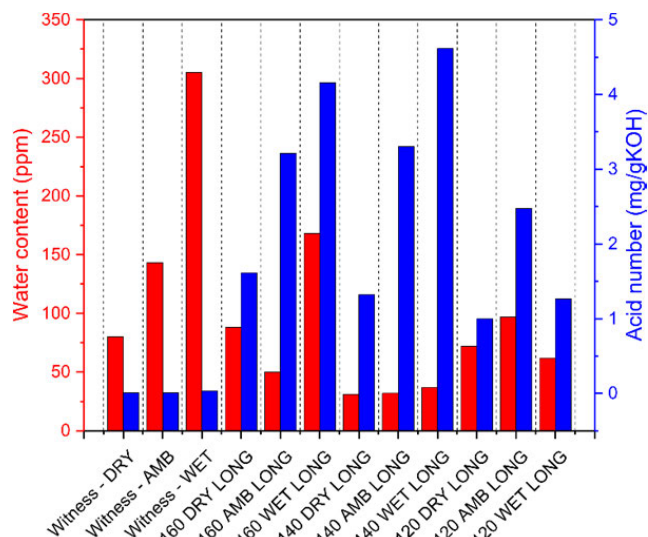


FIGURE 4. Comparison of water content and acid number for each LONG sample.

As seen from the results, dry paper reduced the initial water content of oil from 92 ppm to 80 ppm. The measurement result of the “wet” sample indicates that water is causing the degradation even after a short time and at relatively low temperatures due to the hydrolysis of cellulose (acid number of 0.01 mg/g KOH in the dry witness sample and 0.034 mg/g KOH in the wet witness sample after 800 h at ambient temperature). However, hydrolysis is the predominant reaction [32] in esters at elevated temperatures. More precisely, it is the reaction of natural esters with acids and bases in the presence of water. Hydrolysis can occur only in the presence of water, but this reaction is very unlikely because water is almost unreactive. Acid hydrolysis products are acids (most commonly carboxylic acids) and alcohols (e.g., glycerol). As seen from Figures 3 and 4, at low temperatures, the water content increases due to hydrolysis, while at high temperatures, water is used for ester hydrogenation.

B. DISSIPATION FACTOR AND RELATIVE PERMITTIVITY

The temperature dependence of the dissipation factor of the oil sample was measured as an indicator of aging (Figure 5). As seen from Figures 6 and 7 and comparing with Figures 3 and 4, the results show the dependence of the dissipation factor on the moisture content but does not correspond to aging (comparing the acid number).

In contrast to the results with mineral oil, where the dissipation factor is used as a strong indicator of aging. As seen from Figure 8, the impact of water content and aging on the relative permittivity of a polar natural ester is low, which is expected [33]. However, the low sensitivity of relative humidity to the permittivity [34] has already been monitored for mineral oils.

From the results presented in the previous figures, it can be derived that the dissipation factor cannot be considered as the only indicator of thermal aging in this case.

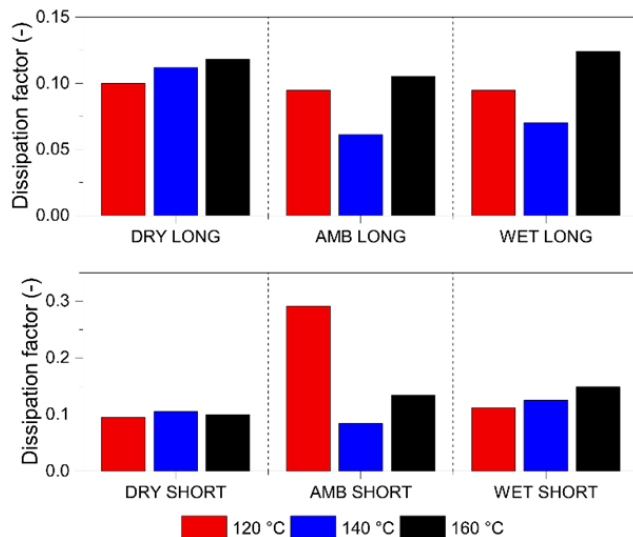


FIGURE 5. Oil dissipation factor measured at 90 °C, with the SHORT and LONG samples.

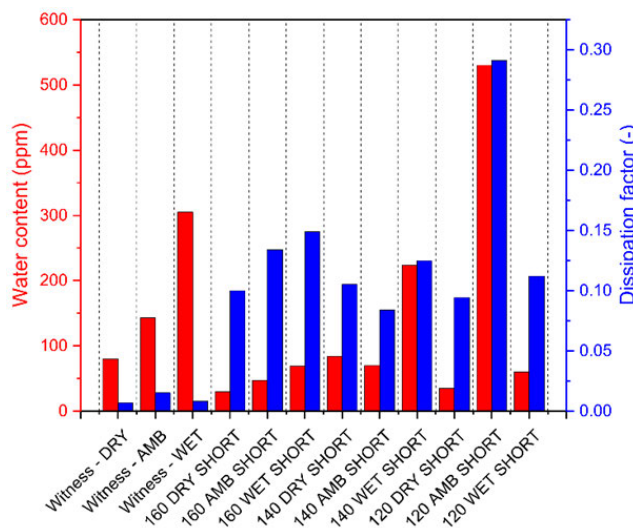


FIGURE 6. Water content in oil and the oil dissipation factor measured at 90 °C for the SHORT samples.

C. BROADBAND DIELECTRIC SPECTROSCOPY

For the characterization of temperature-frequency dependencies, broadband dielectric spectroscopy measurements were performed.

From the results presented in Figure 9, it can be seen that obvious behavior reported, e.g., in [35], is presented only for the “dry” paper, where the conductivity contributes to the dielectric losses. For the “wet” and “ambient” conditions, the dielectric losses are primarily caused by polarization mechanisms (the motion of chain segments or side groups). Depending on the side chain length, the dipolar moment can cause dielectric relaxation along with relaxation of the main chain segment [36].

For this reason, the analysis of polarization mechanisms is shown using generally known Havriliak-Negami

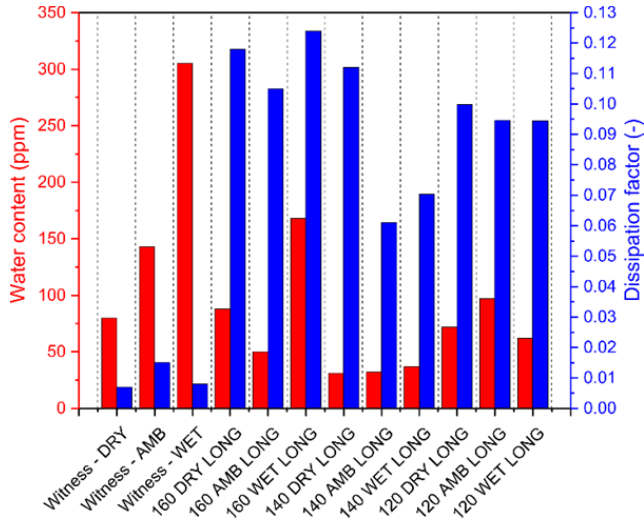


FIGURE 7. Water content in oil and the oil dissipation factor measured at 90 °C for the LONG samples.

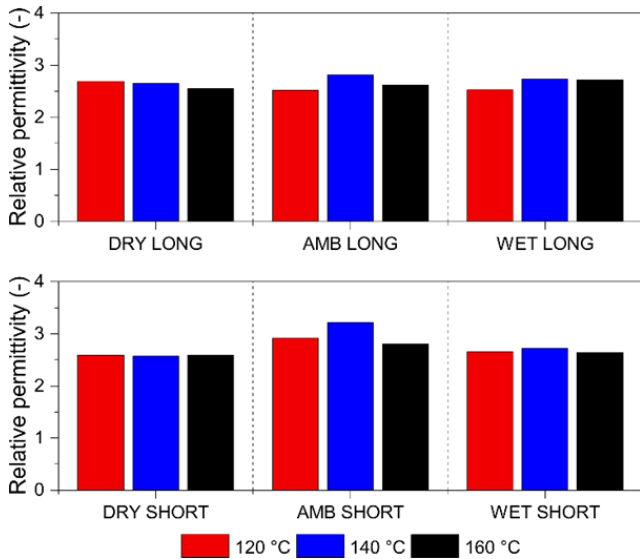


FIGURE 8. Relative permittivity measured at 90 °C with the SHORT and LONG samples.

diagrams [37]. In general, it is preferred to monitor the process of dielectric relaxation in a low-temperature region, where these phenomena are more pronounced and easier to recognize. The results measured at $-30\text{ }^{\circ}\text{C}$ are presented below.

The results show that in the paper-oil insulation system with added moisture, three polarization processes are observed in comparison with that of the “amb” and “dry” conditions (Figures 10, 11, and 12 and Table 5).

The consequence of these FT-IR results is presented in the next paragraph, but the short explanation should be mentioned. In alcohol, OH bonds are polar and exist as hydrogen bridges both between the alcohol molecules themselves and between the alcohol and water molecules. The polarity of the O-H bond causes the formation of partial

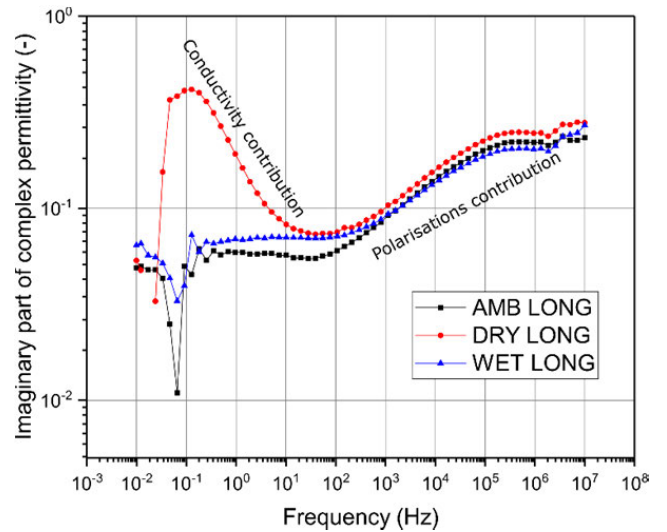


FIGURE 9. Imaginary part of the complex permittivity for the paper samples in oil under LONG conditions at 160 °C and at a measurement temperature of $-30\text{ }^{\circ}\text{C}$.

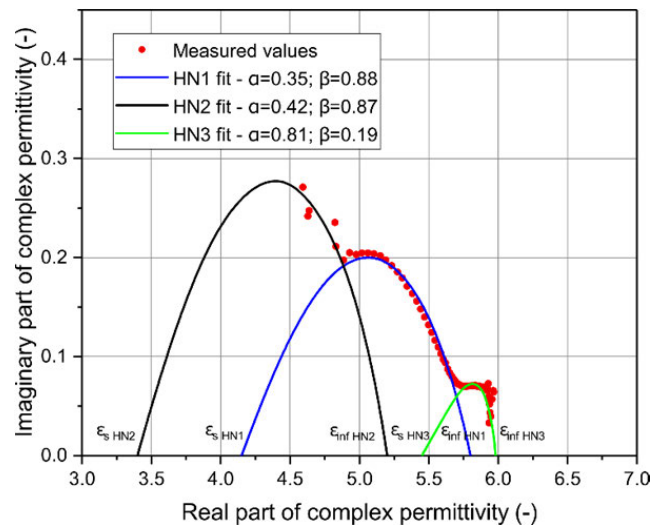


FIGURE 10. H-N diagrams for paper under WET and LONG conditions at 160 °C.

charges on the O (negative) and H (positive) atoms. This results in the acidity of the hydrogen atom of the OH group. The permittivity of ethanol is 24, glycerol is 43, and methanol is 34. The dipole moment of these alcohols is 1.6-1.7 Cm, which allows the formation of a relaxing polarization. This is supported by the measurements shown in Figures 10-12 where two or three relaxation polarizations are observed.

D. INFRARED SPECTROSCOPY

The infrared spectra of the insulating oils were measured by an ATR technique (diamond crystal) using a Nicolet 380 spectrometer. The spectra were acquired over a range of $4000\text{--}400\text{ cm}^{-1}$ at a 4 cm^{-1} resolution with a total of 32 scans co-added for each measured spectrum.

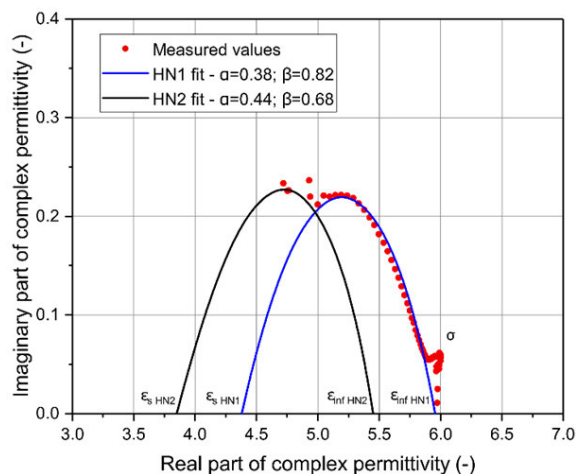


FIGURE 11. H-N diagrams for paper under AMB and LONG conditions at 160 °C.

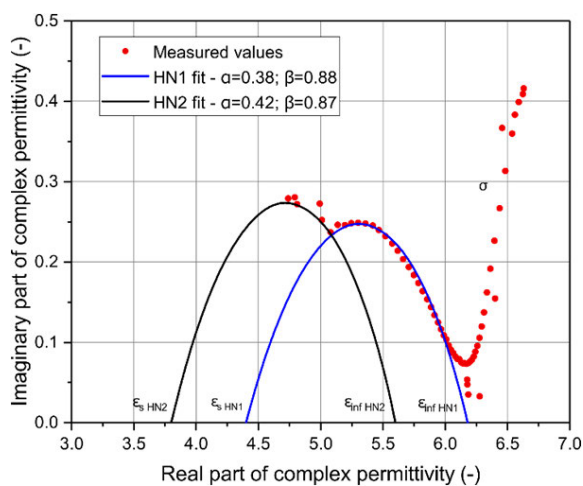


FIGURE 12. H-N diagrams for paper under DRY and LONG conditions at 160 °C.

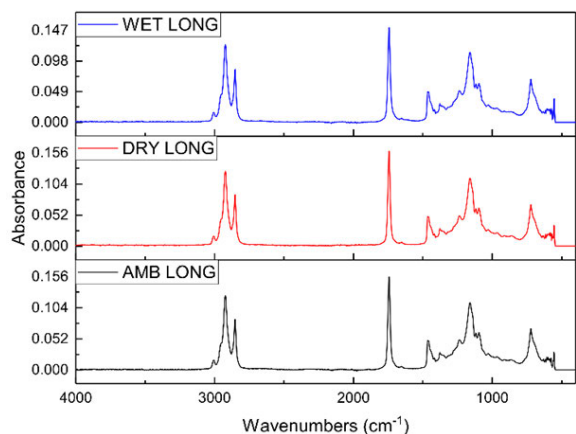


FIGURE 13. FT-IR spectra measured by ATR.

Given the homogeneity of the sample, which ensured a perfect covering of the entire surface of the detection crystal, only one spectrum from each oil sample was measured

TABLE 5. Parameters estimated from the H-N diagrams at a measurement temperature of -30 °C.

| Sample | Fit | α | β | ϵ_s | ϵ_{inf} |
|--------|-----|----------|---------|--------------|------------------|
| WET | HN1 | 0.35 | 0.88 | 5.77 | 4.25 |
| | HN2 | 0.42 | 0.87 | 5.2 | 3.4 |
| AMB | HN1 | 0.81 | 0.19 | 5.98 | 5.45 |
| | HN2 | 0.38 | 0.82 | 5.956 | 4.38 |
| DRY | HN1 | 0.44 | 0.68 | 5.45 | 3.85 |
| | HN2 | 0.38 | 0.88 | 6.17 | 4.4 |
| | HN1 | 0.42 | 0.87 | 3.8 | 5.59 |
| | HN2 | | | | |

where α is a parameter characterizing the relaxation spectrum width ($0 < \alpha < 1$), β is a parameter characterizing the dispersion curve asymmetry ($0 < \beta < 1$),

ϵ_s is the permittivity at $\omega=0$ Hz, and ϵ_{inf} is the permittivity at $\omega=\infty$.

α and β are fitting par. according to the original H-N eq., e.g. in [37]

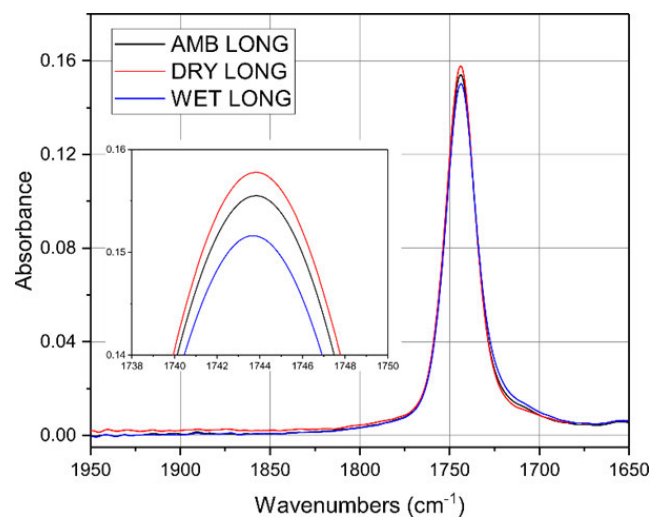


FIGURE 14. Detailed view of the changes at 1740 cm⁻¹.

using this technique. The measured spectra are shown in Figure 13.

The measured natural ester is an unsaturated ester, as evidenced from Figure 13 (data from 3 measurement) by the presence of absorption bands with a maximum at 3009 cm⁻¹ (=C-H stretching symmetric vibration of the cis double bonds) and at 1655 cm⁻¹ (C=C stretching vibration of cis-disubstituted olefins, RHC=CHR) in its spectrum [38]. The FT-IR spectrum also shows some other characteristic absorbance peaks representing vibrations of specific functional groups. According to [39], assignments of the main functional groups of these bands are shown in Table 6, selected detail of changes at 1740 cm⁻¹ presented in Figure 14.

TABLE 6. Wavenumber of functional groups.

| Wavenumber (cm ⁻¹) | Functional group |
|--------------------------------|-----------------------------------------------------------------------------------------------------------------------------|
| 3460 | (C=O) an overtone of C=O of the ester group |
| 3009 | (=C-H) stretching symmetric vibration of the cis double bonds |
| 2926 | (C-H) stretching asymmetric vibration of the aliphatic CH ₂ group |
| 2854 | (C-H) stretching symmetric vibration of the aliphatic CH ₂ group |
| 1747 | (C=O) stretching vibration of the ester carbonyl functional groups of the triglycerides |
| 1655 | (C=C) stretching vibration of the cis-disubstituted olefins |
| 1466 | (C-H) bending vibration of the CH ₂ and CH ₃ aliphatic groups |
| 1397 | (C-H) bending symmetric vibration of the CH ₂ groups |
| 1163 | (C-O-C) stretching vibration of the ester groups |
| 722 | (C-H) rocking vibration of CH ₂ and the out-of-plane vibration of the cis -HC=CH- group of disubstituted olefins |

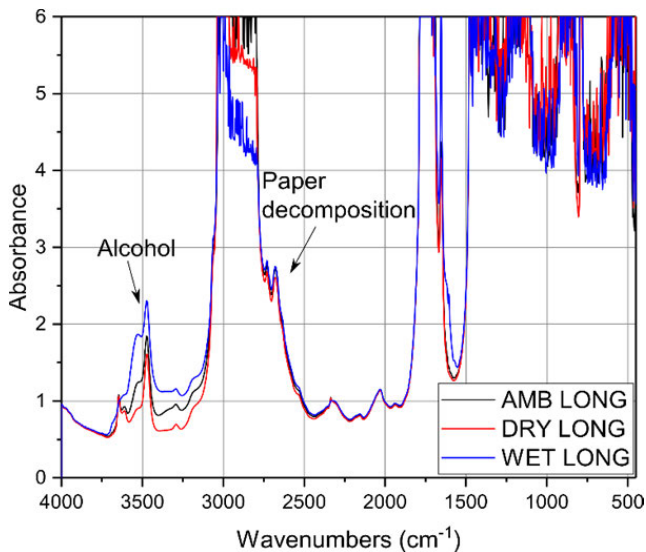


FIGURE 15. Measured spectra by the transmission technique.

We can observe slight differences in the intensity of some bands, especially in the carbonyl region of 1700 – 1800 cm⁻¹ (see Figure 15). The changes in the absorptions in the carbonyl region are still under study. It may be that the changes in the carboxylic acids is due to their utilization by the esterification mechanism versus the generation of new acids due to hydrolysis; the above observation is most likely impossible to discern by infrared or any method since the acids are most likely the same. However, a net reduction in new acids is shown by the depletion of water while at the same time showing a reduction in the acids, as measured

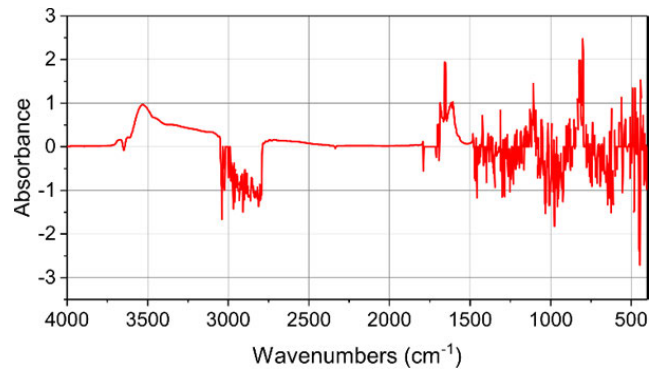


FIGURE 16. Difference spectrum of the DRY and WET oil sample spectra.

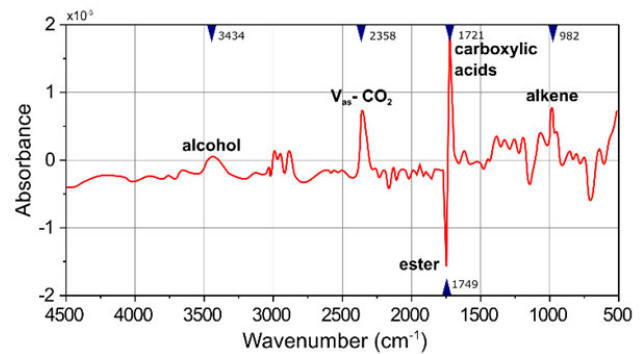


FIGURE 17. Difference spectrum of the natural ester before and after the electrical breakdown (electrical aging), which mainly shows the increase in CO₂ (redrawn and adapted from: [41]).

by the acid value determination; thus the above result offers some hint that the esterification of paper may have taken place.

A further explanation of the cellulose transesterification mechanism is described in [40].

The degradation of the paper is indicated by the significant development of furans and even the CO₂ peak at a wavenumber of 2337 cm⁻¹ (Figures 15 and 17, respectively).

VI. CONCLUSION

This paper is focused on a deeper understanding of the aging mechanism in a paper-natural ester electroinsulating system. The dissipation factor was currently measured as a strong indicator of aging in the power transformer electroinsulating system with mineral oil. From the results (Figures 3 - 7), it can be seen that the dissipation factor cannot be considered as an indicator of the thermal aging in this case. For example, “wet” samples aged at 160 °C for 1200 h show a small increase in tanδ compared to “dry” samples at 160 °C for 1200 h (tanδ = 0.1 vs 0.12, respectively, with both measured at 90 °C), as shown in Figure 5; additionally, tanδ corresponds to the water content, e.g., Figure 6. By studying the acid number, we can see the impact of water on the aging of the samples (an increase from an initial value of 0.01 to a final value of 4.158 mg/g KOH with a “wet” sample, after

1200 h, and a final value of 1.613 mg/gKOH with a “dry” sample). The limit of the acid value according to IEC 62770 is 0.06 mg/g KOH. The water content also cannot be used as an indicator of aging since both hydrolysis and hydrogenation occur during thermal aging. Thus, the results need to be studied more closely with other parameters.

The broadband spectroscopy measurement results and the polarization analysis using H-N diagrams with FT-IR prove that alcohols result from high-temperature degradation. The polar -OH bonds of hydrogen bridges between the alcohol molecules themselves and between the alcohol and water molecules, causes the formation of partial charges on the O (negative) and H (positive) atoms, which causes the acidity of the hydrogen atom in the OH group. The permittivity of alcohols is high (e.g., glycerol 43), with a dipole moment of 1.6-1.7 Cm, which allows the formation of a relaxing polarization (Figures 10-12).

The different aging mechanisms of thermal (hydrolysis and hydrogenation) and electric aging on the formation of CO₂ can be compared in Figures 15-17.

Although some of the aging mechanisms differ in electric insulating systems with minerals and ester oils, the water content plays a key role in the degradation of both systems.

REFERENCES

- [1] I. Fofana, “50 years in the development of insulating liquids,” *IEEE Elect. Insul. Mag.*, vol. 29, no. 5, pp. 13–25, Sep. 2013.
- [2] U. Mohan Rao, I. Fofana, T. Jaya, E. M. Rodriguez-Celis, J. Jalbert, and P. Picher, “Alternative dielectric fluids for transformer insulation system: Progress, challenges, and future prospects,” *IEEE Access*, vol. 7, pp. 184552–184571, 2019.
- [3] I. Fernández, A. Ortiz, F. Delgado, C. Renedo, and S. Pérez, “Comparative evaluation of alternative fluids for power transformers,” *Electr. Power Syst. Res.*, vol. 98, pp. 58–69, May 2013.
- [4] G. De Bellis, L. Calcara, M. Pompili, and M. S. Sarto, “Temperature dependence of the shear viscosity of mineral oils and natural esters,” in *Proc. IEEE 20th Int. Conf. Dielectric Liquids (ICDL)*, Roma, Italy, Jun. 2019, pp. 1–4.
- [5] D. R. Mehta, P. Kundu, A. Chowdhury, V. K. Lakhiani, and A. S. Jhala, “A review on critical evaluation of natural ester vis-a-vis mineral oil insulating liquid for use in transformers: Part I,” *IEEE Trans. Dielectr. Electr. Insul.*, vol. 23, no. 2, pp. 873–880, Apr. 2016.
- [6] D. M. Mehta, P. Kundu, A. Chowdhury, V. K. Lakhiani, and A. S. Jhala, “A review of critical evaluation of natural ester vis-a-vis mineral oil insulating liquid for use in transformers: Part II,” *IEEE Trans. Dielectrics Electr. Insul.*, vol. 23, no. 3, pp. 1705–1712, Jun. 2016.
- [7] M. Bakrtheen, M. W. Iruthayarajan, and S. S. Kumar, “Investigation on the properties of natural esters blended with mineral oil and pyrolysis oil as liquid insulation for high voltage transformers,” in *Intelligent and Efficient Electrical Systems*, M. C. Bhuvanawari and J. Saxena, Eds. Singapore: Springer, 2018, pp. 187–196.
- [8] S. Haegele, F. Vahidi, S. Tenbohlen, K. J. Rapp, and A. Sbravati, “Lightning impulse withstand of natural ester liquid,” *Energies*, vol. 11, no. 8, p. 1964, 2018.
- [9] P. Rozga and M. Stanek, “Characteristics of streamers developing at inception voltage in small gaps of natural ester, synthetic ester and mineral oil under lightning impulse,” *IET Sci., Meas. Technol.*, vol. 10, no. 1, pp. 50–57, Jan. 2016.
- [10] K. Bandara, C. Ekanayake, T. K. Saha, and P. K. Annamalai, “Understanding the ageing aspects of natural ester based insulation liquid in power transformer,” *IEEE Trans. Dielectr. Electr. Insul.*, vol. 23, no. 1, pp. 246–257, Feb. 2016.
- [11] S. Cai, C. Chen, H. Guo, S. Chen, Z. Zhou, and Z. Guo, “Fire resistance test of transformers filled with natural ester insulating liquid,” *J. Eng.*, vol. 2019, no. 16, pp. 1560–1564, Mar. 2019.
- [12] J. Hao, M. Dan, R. Liao, and J. Li, “Effect of moisture on particles accumulation and oil breakdown characteristics in mineral oil and natural ester under non-uniform DC electrical field,” *IEEE Access*, vol. 7, pp. 101785–101794, 2019.
- [13] *Fluids for Electrotechnical Applications-Unused Natural Esters for Transformers and Similar Electrical Equipment*, document IEC 62770:2013, International Electrotechnical Commission, Geneva, Switzerland, 2013.
- [14] *Experiences in Service with New Insulating Liquids; CIGRE Brochure N436*, CIGRE, Paris, France, 2010.
- [15] S. Tenbohlen, M. Jovalekic, L. Bates, and R. Szewczyk, “Water saturation limits and moisture equilibrium curves of alternative insulation systems,” in *Proc. CIGRE SC A2 D1 Joint Colloq.*, Kyoto, Japan, Sep. 2011, pp. 11–16.
- [16] V. Mentlik, P. Trnka, J. Hornak, and P. Totzauer, “Development of a biodegradable electro-insulating liquid and its subsequent modification by nanoparticles,” *Energies*, vol. 11, no. 3, p. 508, 2018.
- [17] T. Heinze, “Cellulose: Structure and properties,” in *Cellulose Chemistry and Properties: Fibers, Nanocelluloses and Advanced Materials*. Cham, Switzerland: Springer, 2015, pp. 1–52.
- [18] Y.-B. Huang and Y. Fu, “Hydrolysis of cellulose to glucose by solid acid catalysts,” *Green Chem.*, vol. 15, no. 5, p. 1095, 2013.
- [19] L. Lundgaard, W. Hansen, and S. Ingebrigtsen, “Ageing of mineral oil impregnated cellulose by acid catalysis,” *IEEE Trans. Dielectr. Electr. Insul.*, vol. 15, no. 2, pp. 540–546, Apr. 2008.
- [20] A. K. Saha and P. Purkait, *Transformer Ageing: Monitoring and Estimation Techniques*. Hoboken, NJ, USA: Wiley, 2017.
- [21] H. J. H. Fenton, “LXXIII.—Oxidation of tartaric acid in presence of iron,” *J. Chem. Soc., Trans.*, vol. 65, no. 1, pp. 899–910, 1894.
- [22] L. Fan, M. M. Gharpuray, and L. Yong-Hyun, *Cellulose Hydrolysis*. Berlin, Germany: Springer-Verlag, 1987.
- [23] I. Pavasars, J. Hagberg, and H. Borén, “Alkaline degradation of cellulose: Mechanisms and kinetics,” *J. Polym. Environ.*, vol. 11, pp. 39–47, Apr. 2003.
- [24] L. Fan, Y.-H. Lee, and D. H. Beardmore, “Mechanism of the enzymatic hydrolysis of cellulose: Effects of major structural features of cellulose on enzymatic hydrolysis,” *Biotechnol. Bioeng.*, vol. 22, no. 1, pp. 177–199, 1980.
- [25] A. J. Varma and M. P. Kulkarni, “Oxidation of cellulose under controlled conditions,” *Polym. Degradation Stability*, vol. 77, no. 1, pp. 25–27, Jan. 2002.
- [26] *Ready Biodegradability; Organisation for Economic Co-operation and Development*, OECD, Paris, France, 1992.
- [27] J. Otera and J. Nishikido, “Reaction of alcohols with carboxylic acids and their derivatives,” in *Esterification: Methods, Reactions, and Applications*. Weinheim, Germany: Wiley, 2010, pp. 3–144.
- [28] B. Garcia, T. Garcia, V. Primo, J. C. Burgos, and D. Urquiza, “Studying the loss of life of natural-ester-filled transformer insulation: Impact of moisture on the aging rate of paper,” *IEEE Elect. Insul. Mag.*, vol. 33, no. 1, pp. 15–23, Jan./Feb. 2017.
- [29] N. Pamuk, “Identification of critical values based on natural ester oils as potential insulating liquid for high voltage power transformers,” *J. Polytch.*, vol. 20, no. 4, pp. 869–877, Dec. 2017.
- [30] T. V. Oommen, “Vegetable oils for liquid-filled transformers,” *IEEE Elect. Insul. Mag.*, vol. 18, no. 1, pp. 6–11, Jan./Feb. 2002.
- [31] J. Silva-Ortega, J. Zapata-Rivera, J. Candelero-Becerra, N. Rosales-Hernández, S. Umaña-Ibáñez, M. Mejia-Taboada, A. Palacio-Bonill, and M. T. Rosas, “Transformadores de distribución que operan con aceite de origen vegetal como dieléctrico y refrigerante,” *INGE CUC*, vol. 12, no. 2, pp. 79–85, 2016.
- [32] K. J. Rapp, C. P. McShane, and J. Luksich, “Interaction mechanisms of natural ester dielectric fluid and kraft paper,” in *Proc. IEEE Int. Conf. Dielectric Liquids (ICDL)*, Coimbra, Portugal, Dec. 2005, pp. 393–396.
- [33] I. S. Darma, “Dielectric properties of mixtures between mineral oil and natural ester,” in *Proc. Int. Symp. Electr. Insulating Mater. (ISEIM)*, Mie, Japan, Sep. 2008, pp. 514–517.
- [34] C. F. Ten, M. A. R. M. Fernando, and Z. D. Wang, “Dielectric properties measurements of transformer oil, paper and pressboard with the effect of moisture and ageing,” in *Proc. Annu. Rep. Conf. Electr. Insul. Dielectr. Phenomena*, Vancouver, BC, Canada, 2007, pp. 727–730.
- [35] M. Dong, M. Ren, F. Wen, C. Zhang, J. Liu, C. Sumereder, and M. Muhr, “Explanation and analysis of oil-paper insulation based on frequency-domain dielectric spectroscopy,” *IEEE Trans. Dielectr. Electr. Insul.*, vol. 22, no. 5, pp. 2684–2693, Oct. 2015.

- [36] A. Rachocki, E. Markiewicz, and J. Tritt-Goc, "Dielectric relaxation in cellulose and its derivatives," *Acta Phys. Polonica A*, vol. 108, no. 1, pp. 137–145, Jul. 2005.
- [37] A. S. Volkov, G. D. Kopusov, R. O. Perfil'ev, and A. V. Tyagunin, "Analysis of experimental results by the Havriliak–Negami model in dielectric spectroscopy," *Opt. Spectrosc.*, vol. 124, no. 2, pp. 202–205, Feb. 2018.
- [38] G. Dombek, Z. Nadolny, and A. Marcinkowska, "Effects of nanoparticles materials on heat transfer in electro-insulating liquids," *Appl. Sci.*, vol. 8, no. 12, p. 2538, 2538.
- [39] N. A. Gomez, R. Abonia, H. Cadavid, and I. H. Vargas, "Chemical and spectroscopic characterization of a vegetable oil used as dielectric coolant in distribution transformers," *J. Brazilian Chem. Soc.*, vol. 22, no. 12, Dec. 2011.
- [40] T. Toudja, F. Chetibi, A. Beldjilali, H. Moulai, and A. Beroual, "Electrical and physicochemical properties of mineral and vegetable oils mixtures," in *Proc. IEEE 18th Int. Conf. Dielectric Liquids (ICDL)*, Bled, Slovenia, Jun./Jul. 2014, pp. 1–4.
- [41] *Environmental Impact Assessment of Transformer Oils and Alternative Insulating Liquids*, Univ. Appl. Sci. Amberg-Weiden, Amberg, Germany, 2019.
- [42] R. Liao, J. Hao, G. Chen, Z. Ma, and L. Yang, "A comparative study of physicochemical, dielectric and thermal properties of pressboard insulation impregnated with natural ester and mineral oil," *IEEE Trans. Dielectr. Electr. Insul.*, vol. 18, no. 5, pp. 1626–1637, Oct. 2011.
- [43] M. M. M. Salama, D.-E.-A. Mansour, M. Daghrah, S. M. Abdelkasoud, and A. A. Abbas, "Thermal performance of transformers filled with environmentally friendly oils under various loading conditions," *Int. J. Electr. Power Energy Syst.*, vol. 118, Jun. 2020, Art. no. 105743.



PAVEL TRNKA (Senior Member, IEEE) received the M.Sc. and Ph.D. degrees from the University of West Bohemia, Czech Republic, in 2002 and 2005, respectively, and the Dr. Habilitation degree from the Faculty of Electrical Engineering, University of Zilina, Slovakia. He was a student of the University of Applied Science, Fachhochschule, Regensburg, Germany, where he was with the Department of Research, Maschinenfabrik Reinhausen, Germany, from 2003 to 2004. From 2006 to 2007, he was a Postdoctoral Associate with the High Voltage Laboratory, Department of Electrical and Computer Engineering, Mississippi State University. He is a DEIS Member and a member of the Executive Committee of the Czechoslovakia Section IEEE. He is the Chairman of CDEE 2020.



IEEE DEIS Member.

JAROSLAV HORNAK (Member, IEEE) was born in Klatovy, in 1989. He received the M.Sc. and Ph.D. degrees from the University of West Bohemia, Czech Republic, in 2014 and 2018, respectively. He completed a traineeship at P&G Rakona, Rakovník, Czech Republic, in 2016, and a practical internship at the Faculty of Electrical Engineering, University of Zilina, Zilina, Slovakia, in 2017. His research interest includes research and development in the area of dielectric materials and diagnostics of their interactions with an electric field. He is the



PAVEL PROSR (Member, IEEE) was born in Susice, Czech Republic, in 1979. He received the M.S. degree in electrical engineering and the Ph.D. degree from the University of West Bohemia, Pilsen, Czech Republic, in 2002 and 2005, respectively. He joined the Department of Technologies and Measurement, University of West Bohemia, in 2005, where he has been working as a Research Worker. He has been a Research and Development Specialist with the Regional Innovation Center for

Electrical Engineering, since 2012. His research interests include the study of the interaction between materials and the environment in electric systems, material diagnostics, and the application of structural analyses in electrical engineering. He is a coauthor of one monograph. He has published more than 170 research articles in journals and conference proceedings.



ONDREJ MICHAL (Member, IEEE) received the master's degree in commercial electrical engineering from the University of West Bohemia, in 2017. Since his bachelor's thesis, he has been specializing in the topic of nanocomposite materials. Within the scope of the project activities, he focuses on new electrical insulation materials for rotating and non-rotating machines, providing a description of their physical properties and diagnostics.



FEIPENG WANG (Member, IEEE) received the Ph.D. degree in materials physics and chemistry from Tongji University, China, in 2007. He was with the Applied Condensed-Matter Physics Group, University of Potsdam, and the Fraunhofer Institute for Applied Polymer Research, Germany, from 2007 to 2013, on topics of functional dielectrics and their applications. He started research with an emphasis on engineering dielectrics and applications in a power grid as a

Professor with Chongqing University, China, in 2014. His research interests include environmentally friendly liquid dielectrics, electrical insulation polymers, functional nanocoatings, nanofibers, and so on. He is also working for the IEEE DEIS as the Co-Chair of the Membership Development and Chapters Committee and as an Editorial Board Member of the *IEEE Electrical Insulation Magazine*. He is a CIGRE 2.69 working Group Member, a Board Member of the IEEE-CEIDP, and a Scientific Committee Member of the IEEE-ICHVE. He will chair the China National Conference on Electrets, in 2020.

• • •